Dab1 and reelin participate in a common signal pathway that controls intestinal crypt/villusunit dynamics

María D. Vá zquez-Carretero, Pablo García-Miranda, María L. Calonge, María J. Peral[1] and Anunciació n A. Ilundain

Departamento de Fisiologı´a, Facultad de Farmacia, Universidad de Sevilla, Spain

Background information. The myofibroblasts placed underneath the epithelium of the rodent small intestine express reelin, and the reelin absence modifies both the morphology and the cell renewal processes of the crypt–villus unit. In the developing central nervous system, the reelin effects are mediated by the disabled-1 (Dab1) protein. The present work explores whether Dab1 mediates the reelin control of the crypt–villus unit dynamics by examining in the mouse small intestine the consequences of the absence of (i) Dab1 (*scrambler* mutation) on crypt–villus unit cell renewal processes and morphology and (ii) reelin (*reeler* mutation) on the intestinal expression of Dab1.

Results. The effects of the *scrambler* mutation on the crypt–villus unit renewal processes are remarkably similar to those caused by the lack of reelin. Thus, both mutations significantly

reduce epithelial cell proliferation, migration and apoptosis, and the number of Paneth cells; affect the morphology of the villus, and expand the intercellular space of the adherens junctions and desmosomes. The Western blot assays reveal that the Dab1 isoform present in the enterocytes has a molecular weight of ~63 kDa and that in the brain of ~82 kDa. They also reveal that the absence of reelin increases Dab1 abundance in both brain and enterocytes.

Conclusions. All together, the current findings link reelin with Dab1 and suggest that Dab1 functions downstream of reelin action on the homeostasis of the crypt–villus unit.

Introduction

The homeostasis of the epithelium of the small intestine is preserved through the strict regula- tion of cell proliferation, growth arrest, migration/ differentiation and apoptosis. Epithelial cells origi- nate from multipotent stem/progenitor cells, located near the bottom of each crypt of Lieberku¨ hn, and cell cycle arrests when cell progenitors reach the crypt–villus junction. As the progeny migrate out of the crypt towards the villus tip, they differentiate in absorptive enterocytes, hormone-secreting enteroen- docrine cells, opioid-producing brush cells, microfoldcells and mucus-producing Goblet cells, and eventu- ally shed into the lumen within less than a week (van der Flier and Clevers, 2009). The antibacte- rial peptide-secreting Paneth cells also arise from the multipotent crypt stem cells, but they migrate to- wards the bottom of the crypt, where they survive for around 6–8 weeks before being eliminated by phago- cytosis (Porter et al., 2002). Spontaneous apoptosis in the crypts is rare and it may serve to remove defec- tive/injured progeny cells and senescent Paneth cells (Potten, 1997).

Epithelial cell turnover and morphogenesis of the small intestine are controlled by cell–cell and cell-underlying basement membrane interactions (Gumbiner, 1996). The nature of cell–basement membrane interactions and their intracellular processing remain largely undefined. Beneath the epithelia are the myofibroblasts, which orchestrate several functions such as the control of epithelial turnover, tissue repair, inflammation and the immune response. They do so by secreting various substances to the extracellular matrix as well as expressing recep- tors for many of them, allowing information flow to and from the intestinal epithelium and the extracel- lular matrix (Andoh et al., 2007; Mifflin et al., 2011). We reported that the myofibroblasts placed underneath the epithelium of the rodent small intes- tine express reelin (Garc´ıa-Miranda et al., 2010) and that reelin absence (*reeler* mutation) modifies both the morphology and the cell renewal processes of the crypt–villus unit (Garc´ıa-Miranda et al.,

2012, 2013). Within the intestinal mucosa, reelin expres- sion is restricted to the myofibroblasts, but both ep- ithelial cells and myofibroblasts express the reelin effector protein disabled-1 (Dab1) (Garc´ıa-Miranda et al., 2010). In the developing central nervous sys- tem, the binding of reelin to its receptors results in tyrosine phosphorylation of Dab1 and in activation of multiple downstream signalling pathway/s, result- ing in cytoskeleton remodelling and precise neuronal positioning (Howell et al., 1999). Whereas the in- formation on the cell signalling cascades initiated by the reelin/Dab1 signalling system in brain is profuse, the studies on the role of reelin/Dab1 in non-neural tissues are scarce. The purpose of the current work was to examine whether Dab1 mediates the observed reelin effects on the crypt–villus unit dynamics. To achieve this, we have examined in mice small in- testine the consequences of (i) Dab1 gene deficiency (*scrambler* mice) on the morphology and on epithe- lial cell proliferation, migration, differentiation and apoptosis and (ii) the absence of reelin (*reeler* mice) on Dab1 expression in the enterocytes. We have used *scrambler* mice because they exhibit a phenotype in- distinguishable from that of the *reeler* mice (Sweet et al., 1996; Sheldon et al., 1997) even though the *scrambler* mice produce about 5% of the normal level of Dab1 protein (Sheldon et al., 1997). A preliminary report of some of these results was published as an abstract (Va´zquez-Carretero et al., 2012).

Results

Weights of the body and small intestine

Dab1-deficient mice (*scrambler*) are used in this study to elucidate whether Dab1 mediates the reelin-induced effects on the crypt–villus unit homeostasis previously reported (Garcia-Miranda et al., 2013). The study was started evaluating body and intestinal weights, as well as intestinal length, of 15 and 60 day-old *scrambler* and control mice. The data sum- marised in Figure 1 reveal that the body weight of the *scrambler* mice is similar to that of the control littermates during the suckling period, but smaller in the 60 day-old mice. The *scrambler* mutation

also decreases both the weight and length of the small intestine at the two ages tested.

Intestinal morphology

In order to determine whether the *scrambler* mutation affects the morphology of the epithelium of the small intestine, the height and width of the villi and the depth and diameter of the crypts were measured in the jejunum and ileum of 15 and 60 day-old control and *scrambler* mice. The results summarised in Table 1 show that the *scrambler* mutation significantly affects the morphology of the villi but not that of the crypts. As compared with control mice, the *scrambler* villi are shorter, mainly in the jejunum, at the two ages tested, and thinner only in the 60 day-old mice.

As the absence of Dab1 reduces the villus length and similarly in the absence of reelin, the cell re- newal processes of the crypt–villus unit are modified (Garc´ıa-Miranda et al., 2012, 2013) we decided to examine the effects of the *scrambler* mutation on ep- ithelial cells to determine whether this mutation also affects epithelial cell proliferation, migration, differ- entiation and apoptosis.

Cell proliferation and migration rates in the epithelium of the small intestine of control and *scrambler* mice

To assess the effects of the *scrambler* mutation on ep-
ithelial cell proliferation and migration rates, the in- corporation of BrdU into DNA was measured in the jejunum and ileum of 15 and 60 day-old control and *scrambler* mice as described in the Materials and Methods section.

Cell proliferation was determined by detecting BrdU-marked cells 90 min after the intraperitoneal injection of the marker. The results are given in Figure 2 and show that, in both types of mice and at the two ages tested, BrdU is only observed in nuclei of the crypt cells. The quantification of the

marked nuclei reveals that the cell proliferation rate is greater in the 60 day-old mice than in the suckling mice in both control and *scrambler* mice. The mutation sig- nificantly reduces the epithelial cell proliferation rate at the two ages and intestinal regions examined by26 2%.

To evaluate the cell migration rate, intestinal BrdU-marked cells were detected 32 h after injection of the marker and the results are shown in Figure 3. In both types of mice, the cell migration rate along the villi is greater in the 60 day-old mice than in the suckling mice and it is significantly reduced by the mutation in all the experimental conditions tested by34 ± 4%.

Cell apoptosis in the epithelium of the small intestine of control and *scrambler* mice

Cell apoptosis was evaluated by immunological detection of cleaved Caspase-3 in the jejunum and ileum of 15 and 60 day-old control and *scrambler* mice. The anti-cleaved Caspase-3 antibody detects on a West- ern blot a band of 17 kDa that is indicative of cell apoptosis (see Figure 4A). The immunohistochem- istry assay reveals that in both control and *scrambler* mice the apoptotic cells are mainly observed at the villus (Figure 4C). In control mice, both the den- sity of the 17-kDa band (Figure 4A) and the number of apoptotic cells (Figure 4B) are higher in the 60 day-old than in the 15 day-old mice. The *scrambler* mutation decreases the density of the band (42 5% decrease) and the number of apoptotic cells (59 4% decrease) in all the experimental conditions tested.

Cell differentiation in the epithelium of the small intestine of control and *scrambler* mice

Epithelial cell differentiation was evaluated by measuring the number of Goblet and Paneth cells in the jejunum and ileum of 15 and 60 day-old control and *scrambler* mice. Goblet cells were identified by the periodic acid- Shiff (PAS)

staining system, as described in Materials and Methods section, and Figure 5 shows that the number of PAS positive cells increases with the age in both types of mice. The *scrambler* mutation decreases the number of Goblet cells, mainly in the 15 day-old jejunum. No significant differences are observed in the 60 day-old jejunum. Paneth cells were quantified by immuno-detection of lysozyme and the results are summarised in Figure 6. They reveal that age increases the number of Paneth cells in both control and *scrambler* mice and that the mutation reduces their number at the two ages and intestinal regions examined by 29,3%.

Electron microscopy studies

The results discussed so far reveal that the *scrambler* mutation reduces epithelial cell proliferation, migra- tion, differentiation and apoptosis. Because intercellular junctions control these processes (Gumbiner, 1996; Herve´, 2009) and the *reeler* mutation affects those junctions in the intestinal epithelium (Garc´ıa- Miranda et al., 2013), the effects of the *scrambler* mu- tation on the cell-to-cell junctions were examined at the electron microscopy. In the intestinal epithelium, the intercellular junctions are located on the apical side of the lateral cell membrane and form the api- cal junctional complex that comprises tight junctions (TJ), adherens junctions (AJ) and desmosomes. The microphotographs of Figure 7 reveal that the TJ appear normal, but the intercellular space of both the AJ and desmosomes is significantly wider in the *scrambler* than in the control mice.

Immunolocalisation of E-cadherin and *β*-catenin in the epithelium of the small intestine of control and *scrambler* mice

Since the electron microscopy studies revealed that the *scrambler* mice present AJ with wider intercellular space than the control mice, the cell location of E-cadherin in the epithelium of the control and *scrambler* small intestine was detected by immuno- histochemistry (Figure 8). *β*-catenin associates with the cytosolic domain of the E-cadherin and regulates several cell processes. As its cell membrane location in part depends on the amount of E-cadherin present in the cell membrane, *β*-catenin localisation was also investigated by immunostaining in both types of mice (Figure 8). The specific signal produced by the

anti-E- cadherin antibody is seen at the lateral membrane of the epithelial cells in both control and *scrambler* mice. *β*-Catenin-specific staining is also concentrated at the lateral cell membrane. No significant differences be- tween the two types of mice are observed, indicating that the mutation does not modify the cell location of either protein. Immunoreactive signal was not seen in the absence of the primary antibodies (data not shown).

Dab1 protein in enterocytes isolated from control, *reeler* and *scrambler* mice

The last set of experiments was designed to (i) deter- mine the Dab1 isoform expressed in mice enterocytes,(ii)compare the intestinal isoform with that expressed in brain and (iii) determine whether reelin modifies the intestinal expression of Dab1. This was done by Western blot assays using an anti-Dab1 antibody raised against the C terminus of Dab1 that recognises all Dab1 isoforms. The specificity of the antibody was verified using brain and enterocytes isolated from the *scrambler* mice, which should show drastic reduction in Dab1 expression on a Western blot. The results are given in Figure 9A. The bands detected by the anti-Dab1 antibody that is absent in the *scrambler* tissues are a polypeptide band at ~63 kDa in the enterocytes and a polypeptide of ~82 kDa in the brain.

To test whether reelin modifies the expression of Dab1 its abundance was measured in enterocytes isolated from control and *reeler* mice. Figure 9A shows that the *reeler* mutation increases Dab1 abundance by a factor of approximately 2 relative to control in both enterocytes and brain.

The Western blot does not provide evidence on the subcellular location of Dab1, which was investigated by immunocytochemistry. Figure 9B reveals that the specific signal produced by the anti-Dab1 antibody is seen throughout the cytosol, and in some cells the signal is stronger at the terminal web domain. The specific labelling was absent from the enterocytes isolated from *scrambler* mice.

Discussion

The reelin-signalling system and its role in tissues other than the brain is poorly understood. We re- ported that in the rodent small intestine reelin is released by the myofibroblasts placed underneath the epithelium and involved in the homeostasis of the crypt–villus unit (Garc´ıa-Miranda et al., 2010, 2012, 2013). The current work extends the knowledge of the reelin-signalling system by revealing that in the small intestine Dab1 also might transmit the reelin signal to cytosolic signalling pathway/s, which ultimately might affect the cell renewal processes of the crypt–villus unit. As compared with the brain, mouse enterocytes express significant amounts of Dab1 and a different Dab1 isoform: the enterocyte isoform is ~63 kDa and that in the brain ~82 kDa. Both the size of the bands and the differences between brain and enterocytes are consistent with the high diversity observed in Dab1 expression. Dab1 polypeptide bands ranging from 36 to 120 kDa have been identified in mouse embryonic brain, the 80-kDa Dab1 being the predominant form (Howell et al., 1997). It has also been reported that the Dab1 forms resulting from alternative splicing are species specific, have different tissue expression pro- files and sometimes are expressed in the same tissue at the same stage of development or in different sub-populations of cells depending on the stage of development (Bar et al., 2003; Katyal and Godbout, 2004; Costagli et al., 2006; Gao et al., 2010; Long et al., 2011; Gao et al., 2012). The physiological meaning of the differing presence of a Dab1 isoform in the small intestine from that in brain is unclear at present. The molecular weight of the intestinal isoform is close to that of the “Dab1 early (Dab1-E) isoform” expressed in the progenitor cells of the human/chicken retina and chicken embryos gut (Gao et al., 2010; Katyal et al., 2011). A “late (Dab1-L) isoform” (commonly referred to as Dab1) has been isolated from differentiating retinal cells (Gao et al., 2010). The Dab1-E is missing two tyrosine

phosphorylation sites critical for Reelin-Dab1 signalling and, consequently, reelin can activate the signalling cascade only in cells expressing Dab1-L (Gao et al., 2010). In the intestinal epithelium, there are proliferating (crypts) and differentiated (villi) cells exposed to the reelin secreted by the myofibroblasts but only one intestinal Dab1 isoform is detected on a Western blot. The intestinal Dab1 form seems to be linked to reelin because, as in brain (Sheldon et al., 1997; Rice et al., 1998; Howell et al., 1999), the *reeler* mutation increases Dab1 abundance (current observations), without affecting Dab1mRNA levels (García-Miranda et al., 2013). This has been interpreted as the requirement of reelin for Dab1 degradation (Arnaud et al., 2003; Bock et al., 2004).

Observations supporting the view that in the small intestine reelin and Dab1 proteins are linked are those showing that both, *scrambler* and *reeler* (Garc´ıa- Miranda et al., 2013) mutations induce extremely similar changes on the morphology of the villi, on the dynamics of the crypt–villus axis and on the structure of apical junctions. The reduction in the size of the villi could result from the mutation-induced changes on the dynamics of the crypt–villus axis. Thus the de- crease in the cell proliferation in the crypts suggests that Dab1 stimulates stem cells. The decrease in the cell proliferation rate might explain the observed decrease in cell migration along the crypt–villus axis. An increase in apoptosis in the crypts could also slow migration by decreasing the number of cells exiting the crypts towards the villus. This does not appear to be the case because apoptotic cells are only observed at the villi tip. The length of the villi is also deter- mined by apoptosis at the villi, which is decreased in the *scrambler* mice. All these observations support the view that the reelin/Dab1-signalling system has a growth-promoting action in the small intestine. Both, *reeler* and *scrambler* mutations also reduced the number of Paneth cells (Garc´ıa-Miranda et al., 2013 and current observations), but they have opposing effects on the numbers of Goblet cells: the number of Goblet cell was either

unaffected or increased in the 60 day-old mice by the *reeler* mutation (García- Miranda et al., 2013) but is marginally decreased in *scrambler* mice. The physiological meaning of the differences between Goblet and Paneth cells might indicate that the two cell lineages have different re- quirements for their differentiation. The capacity of reelin and Dab1 to regulate cell proliferation, migra- tion and differentiation in the small intestine agrees with observations made in neural (Sheldon et al., 1997; Rice et al., 1998; Massalini et al., 2009) and non-neural tissues (Khialeeva et al., 2011).

Adhesion junctions maintain tissue integrity and epithelial homeostasis, and both *reeler* and *scrambler* mutations expand the intercellular space of the AJ and desmosomes, without modifying the TJ (García- Miranda et al., 2013 and current observations). The latter is corroborated by the lack of effect of the *reeler* mutation on TJ permeability (Garc´ıa-Miranda et al., 2013). The reelin/Dab1-related expansion of the junctions does not seem to be due to mislocalisation of E-cadherin at the lateral membrane of epithelial cells, because neither *reeler* (Garc´ıa- Miranda et al., 2013) nor the *scrambler* mutation (current observations) affects the cell membrane location of E-cadherin. Neither the membrane location of *β*-catenin, which in part depends on the amount of E-cadherin present in the membrane, is modified by the *scrambler* mutation. These observations suggest that the mutations-induced expansion of intercellular space of the adherens and desmosomes junctions might result from changes in the dynamics of the actin cytoskeleton.

The downstream signalling pathways modified by reelin/Dab1 in non-neural tissues remain un- revealed. In the intestine, the *reeler* mutation af- fects the expression of genes coding for proteins that inhibit epithelial cell proliferation, migration and apoptosis (Garc´ıa-Miranda et al., 2012). Among them, let us mention the down-regulation of *β1- arrestin*. In the small intestine, *β*1-arrestin activates the actin-depolymerising factor/cofilin (Lau et al., 2011) and it is a necessary

component of the Wnt/*β*- catenin system (Bryja et al., 2007), which induces intestinal cell proliferation (Bryja et al., 2007) and controls the number of Paneth cells (Yeung et al., 2011). Therefore, the *reeler*-induced down-regulation of *β1-arrestin* would modify cell events that depend on the actin cytoskeleton, such as the structure of the apical junctions, as well as cell proliferation, migration and differentiation.

The observations discussed so far indicate that Dab1 could transmit the reelin signal to downstream signalling pathway/s. In the small intestine, reelin expression is restricted to the myofibroblasts located underneath the epithelium. Therefore, reelin can only signal the enterocytes through their basal membrane and the Dab1 activated by reelin must be near this membrane. However, as observed in intact tissue (García-Miranda et al., 2010), Dab1 is distributed throughout the enterocyte cytosol and in some cells the specific labelling is stronger at their terminal web domain. This cell distribution might indicate that Dab1, once activated by reelin, migrates from the basal to the apical domain of the epithelial cells. Alternatively, the apical Dab1 might mediate reelin independent processes, such as apical endo/exocytosis processes (Bento-Abreu et al., 2009) and even act as a nucleo-cytoplasmic shuttling protein (Honda and Nakajima, 2006; Martín-López et al., 2011).

In conclusion, the current work provides evidence suggesting that reelin and Dab1 participate in a common signal pathway that controls intestinal crypt–villus unit dynamics. How the reelin/Dab1- signalling system controls epithelial homeostasis re-mains to be elucidated.

Materials and methods

The antibodies: anti-cleaved Caspase-3 (Asp175) was obtained from Cell Signaling; anti-Dab1 (PA1–26899) from ABR Affinity Bio Reagents; anti-Dab1 (ab67104) from AbCam; anti- lysozyme (EC 3.2.1.17) from Dako; anti-E-cadherin

(6110181) and anti-*β*-catenin from BD Transduction Laboratories; anti- BrdU (B2531) and anti-*β*-actin (AC-15) from Sigma-Aldrich. Unless otherwise stated, the other reagents were obtained from Sigma-Aldrich, Spain.

Animals

Control (wild-type), *reeler* and *scrambler* mice of 15 and 60 day-old were used. *Reeler* (*rl*) and *scrambler* (*scm*) are spontaneous autosomal recessive mutation of reelin (D'Arcangelo et al., 1995) and Dab1 (Sheldon et al., 1997), respectively. Heterozygous (*rl*$^{+}$/*rl*$^{-}$) (C57BL/6) and (*scm*$^{+}$/*scm*$^{-}$) (DC/LeJ) mice were purchased from Jackson Laboratories (Bar Harbor, ME, USA), through Charles River Laboratories, Spain. Control (*rl*$^{+}$/*rl*$^{+}$, *scm*$^{+}$/*scm*$^{+}$) and homozygous *reeler* (*rl*$^{-}$/*rl*$^{-}$) and *scrambler* (*scm*$^{-}$/*scm*$^{-}$) mice were obtained by heterozygous crossings, as described (D'Arcangelo et al., 1996; Usman et al., 2000). The animals were housed in a 12:12 light-dark cycle and fed *ad libitum* with Global 2019 extruded rodent diet (Harlan Ibe´rica S.L.) with free access to tap water. Mice were genotyped by PCR analysis of genomic DNA, using the primers (5^{r}-3^{r}) TAATCTGTCCTCACTCTGCC, CAGTTGACATACCTTAAT and TGCATTAATGTGCAGTGT for the *reeler* and TTTTGTCCTTCTCTATAACT, CCTGGGATAATGGGGTAAG and AGCAGCGAACTCAGTACAACA, for the *scrambler* mice. The mice were humanely handled and sacrificed by cervical dislocation in accordance with the European Council legislation 86/609/EEC concerning the protection of experimental animals.

Morphological studies

The small intestine was rapidly removed from the mice, washed with ice-cold saline solution and fixed by incubation with PBS containing 4% paraformaldehyde at 4°C overnight. 10 µm cryosections were stained with hematoxylin and eosin procedure. Measurements of villi (height and width) and crypts (diameter and depth) parameters were done on at least 30 well oriented full length crypt–villus units per animal. Morphometry was performed using a Zeiss Axioskop 40 microscope equipped with a SPOT Insight V 3.5 digital camera. Acquired images were analysed by using Spot Advance 3.5.4.1 Program analysis (Diagnostic Instrument, Inc.). Three independent observers made the measurements.

Immunostaining analysis

Immunostaining assays were performed on intact small intestine (10 µm cryosections or 5 µm paraffin sections) and on isolated intestinal cells, as previously (Garcia-Miranda et al., 2010). The slides containing either the intestinal sections or the isolated cells were incubated with the indicated primary anti- body at 4°C, overnight. Antibody binding was visualised with biotinylated anti-IgG antibodies, at dilution 1:100, followed by immunoperoxidase staining. The Vectastain ABC peroxidase kit (Vector) and 3,3'-diaminobenzidine were used. Controls were carried out without primary antibody. The slides were rinsed, mounted and photographed as indicated above.

Western assays

SDS-PAGE was performed on either a 7.5% or 15% polyacrylamide gel as described (Peral et al., 2002). Protein was extracted from the enterocytes and brain as described (Garcia-Miranda et al., 2013) and it was measured by the Bradford method (Brad- ford, 1976) using gamma globulin as the standard. A total of 50 µg protein was loaded to each lane. The immunoreactive bands were viewed using a chemiluminescence procedure (GE Health- care). Anti-β-actin antibody (1:3000 dilution) was used to normalise band density values. The relative abundance of the bands was quantified using ImageJ program version 1.46 (National Institutes for Health, http://rsb.info.nih.gov/ij/index.html).

Crypt cell proliferation and migration rate

Mice received an intraperitoneal injection of 5-bromo deoxyuridine (BrdU) (120 mg/Kg body weight). The BrdU incorporated into DNA was detected by immunohistochemistry using a monoclonal anti-BrdU antibody, 1:300 dilution, as described above. For epithelial cell proliferation measurements, mice were sacrificed 90 min after the

intraperitoneal injection. The number of BrdU-labelled cells in 30 crypts well oriented longitudinally per mouse was determined by light microscopy by three independent observers. The crypt cell proliferation rate is expressed as the number of BrdU-positive cells per crypt.

The cell migration rate was estimated by measuring the distance from the base of the villus to the foremost labelled cell at 32 h after injection of BrdU. Thirty villi well oriented longitudinally per mouse were used, and three independent observers made the measurements. The cell migration rate is expressed as µm/h.

Evaluation of cell apoptosis

Apoptosis in the epithelium of the small intestine was evaluated by immunological detection (Western blot and immunohistochemistry assays) of cleaved Caspase-3. A polyclonal anti-cleaved Caspase-3 antibody was used at dilution 1:1000 for the Westerns and at dilution 1:200 for immunohistochemistry. The number of labelled cells in 200 well oriented longitudinally villi per mouse was determined by light microscopy by three independent observers. Results are expressed as the number of labelled cells per 40 villi.

Goblet cells staining

The PAS staining system was used to identify and quantify the Goblet cells in the epithelium of the small intestine. The number of labelled cells, in 30 villi well oriented longitudinally per mouse, was determined by three independent observers. The results are expressed as the number of Goblet cells per villus.

Paneth cells staining

Paneth cells were quantified by lysozyme detection using a poly- clonal anti-lysozyme antibody (DAKO; 1:200 dilution). The number of labelled cells, in 30 crypts well oriented longitudinally per mouse, was determined by three independent observers.

The results are given as the number of positive lysozyme cells per crypt.

Electron microscopy assays

Segments of small intestine were fixed in 4% glutaraldehyde/0.1 mol/l sodium cacodylate, pH 7.4 at 4°C for 3 h. After three rinses in cacodylate-buffered solution, the tissues were postfixed in 1% OsO_4 in 0.1 M phosphate buffer at 4°C for 1 h and washed in cacodylate-buffered solution containing 7.5% sucrose. The segments were then dehydrated in a graduated series of acetone (30%, 50% and 70%), stained with 2% uranyl acetate and embedded in Spurr's epoxy resin. Ultrathin sections were examined under a Philips CM-10 trans- mission electron microscope equipped with an Olympus Veleta. The photographs were processed with iTEM software and ImageJ program version 1.46 (National Institutes for Health, http://rsb.info.nih.gov/ij/index.html).

Statistical analysis

Data are presented as mean SEM. The number of animals is indicated in the legends. In Figures 7 and 9 comparisons between different experimental groups were evaluated by the two-tailed Student's *t* test. One-way ANOVA followed by the Newman– Keuls' test was used for multiple comparisons (GraphPad Prism program). Differences were set to be significant for $P < 0.05$.

Author contribution

M.J.P. and A.A.I. conceived and designed the experiments. M.D.V-C, P.G-M. and M.L.C. performed the experiments. M.J.P., M.L.C. and A.A.I. analysed and interpreted the data. A.A.I. carried out the discussion and wrote the paper.

Acknowledgements

We thank Dr. O. Pintado (Centro de Producción y Experimentación Animal, Universidad de Sevilla), Dr. L. Collinson (Cancer Research Institute of Lon- don), Dr. F. Romero and Dr. N. Wright's laboratory (Cancer Research Institute of

London) for their technical advice and R. Caracuel for technical sup- port The anti-lysozyme and anti-β-catenin antibodies were kindly gifted by Dr. N. Wright. Electron- microscopy images were obtained in the Centro de Investigación, Tecnología e Innovación, Universidad de Sevilla.

Funding

This work was supported by a grant from the Junta de Andalucia (CTS 884) and by a fellowship from the Spanish Ministerio de Educación y Ciencia (AP2007- 04201) to M.D. Vazquez-Carretero.

Conflict of interest statement

The authors have declared no conflict of interest.

References

Andoh, A., Bamba, S., Brittan, M., Fujiyama, Y. and Wright, N.A. (2007) Role of intestinal subepithelial myofibroblasts in inflammation and regenerative response in the gut. Pharmacol. Ther. **114**, 94–106

Arnaud, L., Ballif, B.A. and Cooper, J.A (2003). Regulation of protein tyrosine kinase signaling by substrate degradation during brain development. Mol. Cell Biol. **23**, 9293-9302

Bar, I., Tissir, F., Lambert de Rouvroit, C., De Backer, O. and Goffinet, A.M. (2003) The gene encoding disabled-1 (DAB1), the intracellular adaptor of the Reelin pathway, reveals unusual complexity in human and mouse. J. Biol. Chem. **278**, 5802–5812

Bento-Abreu, A., Velasco, A., Polo-Hernandez, E., Lillo, C., Kozyraki, R., Tabernero, A. and Medina, J.M. (2009) Albumin endocytosis via megalin in astrocytes is caveola- and Dab-1 dependent and is required for the synthesis of the neurotrophic factor oleic acid. J. Neurochem. **111**, 49–60

Bradford, M.M. (1976) A rapid and sensitive method for the quantitation of microgram quantities of protein utilizing the principle of protein-dye binding. Anal. Biochem. **72**, 248–254

Bock, H.H., Jossin, Y., May, P., Bergner, O. and Herz, J. (2004) Apolipoprotein E receptors are required for reelin-induced proteasomal degradation of the neuronal adaptor protein Disabled-1. J. Biol. Chem. **279**, 33471–33479

Bryja, V., Grad, l.D., Schambony, A., Arenas, E. and Schulte, G. (2007) Beta-arrestin is a necessary component of Wnt/beta-catenin signaling in vitro and in vivo. Proc. Natl. Acad. Sci. USA. **104**, 6690–6695

Costagli, A., Felice, B., Guffanti, A., Wilson, S.W. and Mione, M. (2006) Identification of alternatively spliced dab1 isoforms in zebrafish. Dev. Genes Evol. **216**, 291–299

D'Arcangelo, G., Miao, G.G. and Curran, T. (1996) Detection of the reelin breakpoint in *reeler* mice. Brain Res. Mol. Brain Res. **39**, 234–236

D'Arcangelo, G., Miao, G.G., Chen, S.C., Soares, H.D., Morgan, J.I. and Curran, T. (1995) A protein related to extracellular matrix proteins deleted in the mouse mutant *reeler*. Nature **374**, 719–723

Gao, Z., Monckton, E.A., Glubrecht, D.D., Logan, C. and Godbout, R. (2010) The early isoform of disabled-1 functions independently of Reelin-mediated tyrosine phosphorylation in chick retina. Mol. Cell Biol. **30**, 4339–4353

Gao, Z., Poon, H.Y., Li, L., Li, X., Palmesino, E., Glubrecht, D.D., Colwill, K., Dutta, I., Kania, A., Pawson, T. and Godbout, R. (2012) Splice-mediated motif switching regulates disabled-1 phosphorylation and SH2 domain interactions. Mol. Cell Biol. **32**, 2794–2808

Garcıa-Miranda, P., Peral, M.J. and Ilundain, A.A. (2010) Rat small intestine expresses the reelin-disabled-1 signalling pathway. Exp.

Physiol. **95**, 498–507

Garcıa-Miranda, P., Vazquez-Carretero, M.D., Gutierrez, G., Peral, M.J., and Ilunda´ in, A.A. (2012) Lack of reelin modifies the gene expression in the small intestine of mice. J. Physiol. Biochem. **68**, 205–218

Garcıa-Miranda, P., Vazquez-Carretero, M.D., Sesma, P., Peral, M.J. and Ilundain, A. A. (2013) Reelin is involved in the crypt-villus unit homeostasis. Tissue Eng. **19**, 188–198

Gumbiner, B.M. (1996). Cell adhesion: the molecular basis of tissue architecture and morphogenesis. Cell **84**, 345–357

Herve , J.C. (2009). The apical junctional complexes, roles, and dysfunctions. Biochim. Biophys. Acta **1788**, 753–754

Honda, T. and Nakajima, K. (2006) Mouse Disabled1 (DAB1) is a nucleocytoplasmic shuttling protein. J. Biol. Chem. **281**,38951–38965

Howell, B.W., Gertler, F.B. and Cooper, J.A. (1997) Mouse disabled (mDab1): a Src binding protein implicated in neuronal development. EMBO J. **16**, 121–132

Howell, B.W., Herrick, T.M. and Cooper, J.A. (1999) Reelin-induced tyrosine phosphorylation of Disabled 1 during neuronal positioning. Genes Dev. **13**, 643–648

Katyal, S., Glubrecht, D.D., Li, L., Gao, Z. and Godbout, R. (2011) Disabled-1 alternative splicing in human fetal retina and neural tumors. PLoS One **6**, e28579

Katyal, S. and Godbout, R. (2004) Alternative splicing modulates Disabled-1 (Dab1) function in the developing chick retina. EMBO J. **23**, 1878–1888

Khialeeva, E., Lane, T.F. and Carpenter, E.M. (2011) Disruption of reelin signaling alters mammary gland morphogenesis. Development **138**, 767–776

Lau, C., Lytle, C., Straus, D.S. and DeFea, K.A. (2011) Apical and basolateral pools of proteinase-activated receptor-2 direct distinct signaling events in the intestinal epithelium. Am. J. Physiol. Cell Physiol. **300**, C113–C123

Long, H., Bock, H.H., Lei, T., Chai, X., Yuan, J., Herz, J., Frotscher, M. and Yang, Z. (2011) Identification of alternatively spliced Dab1 and Fyn isoforms in

pig. BMC Neurosci. **12**, 17–31

Martın-Lopez, E., Blanchart, A., De Carlos, J.A. and Lopez-Mascaraque, L. (2011) Dab1 (Disable homolog-1) reelin adaptor protein is overexpressed in the olfactory bulb at early postnatal stages. PLoS One **6**, e26673

Massalini, S., Pellegatta, S., Pisati, F., Finocchiaro, G., Farace, M.G. and Ciafre, S.A. (2009) Reelin affects chain-migration and differentiation of neural precursor cells. Mol. Cell Neurosci. **42**, 341–349

Mifflin, R.C., Pinchuk, I.V., Saada, J.I. and Powell, D.W. (2011)Intestinal myofibroblasts: targets for stem cell therapy. Am. J. Physiol. Gastrointest. Liver Physiol. **300**, G684-G696

Peral, M.J., Garcıa-Delgado, M., Calonge, M.L., Dura´ n, J.M., De La Horra, M.C., Wallimann, T., Speer, O. and Ilundain, A.A. (2002) Human, rat and chicken small intestinal Na^+–Cl^--creatine transporter: functional, molecular characterization and localization.J. Physiol. **545**, 133–144

Porter, E.M., Bevins, C.L., Ghosh, D. and Ganz, T. (2002) The multifaceted Paneth cell. Cell. Mol. Life Sci. **59**, 156–170

Potten, C.S. (1997) Epithelial cell growth and differentiation. II. Intestinal apoptosis. Am. J. Physiol. **273**, 253–257

Rice, D.S., Sheldon, M., D'Arcangelo, G., Nakajima, K., Goldowitz, D. and Curran, T. (1998) Disabled-1 acts downstream of Reelin in a signaling pathway that controls laminar organization in the mammalian brain. Development **125**, 3719–3729

Sheldon, M., Rice, D.S., D'Arcangelo, G., Yoneshima, H., Nakajima, K., Mikoshiba, K., Howell, B.W., Cooper, J.A., Goldowitz, D. and Curran, T. (1997) Scrambler and yotari: disrupt the disabled gene and produce a *reeler*-like phenotype in mice. Nature **389**, 730–733

Sweet, H.O., Bronson, R.T., Johnson, K.R., Cook, S.A. and Davisson, M.T. (1996) Scrambler, a new neurological mutation of the mouse with abnormalities of neuronal migration. Mamm. Genome. **7**, 798–802

Usman, N., Tarabykin, V. and Gruss, P. (2000) The novel PCR-based technique of genotyping applied to identification of *scrambler* mutation

in mice. Brain Res. Brain Res. Protoc. **5**, 243–247

van der Flier, L.G. and Clevers, H. (2009) Stem cells, self-renewal, and differentiation in the intestinal epithelium. Annu. Rev. Physiol. **71**, 241–260

Vazquez-Carretero, M.D., Garcıa-Miranda, P., Calonge, M.L., Calvo, E., Lopez, J.A., Romero, F., Ilundain, A.A. and Peral, M.J. (2012) Disabled-1 protein in the intestine. Genes Nutr. **6**, S75

Yeung, T.M., Chia, L.A., Kosinski, C.M. and Kuo, C.J. (2011) Regulation of self-renewal and differentiation by the intestinal stem cell niche. Cell. Mol. Life Sci. **68**, 2513–2523

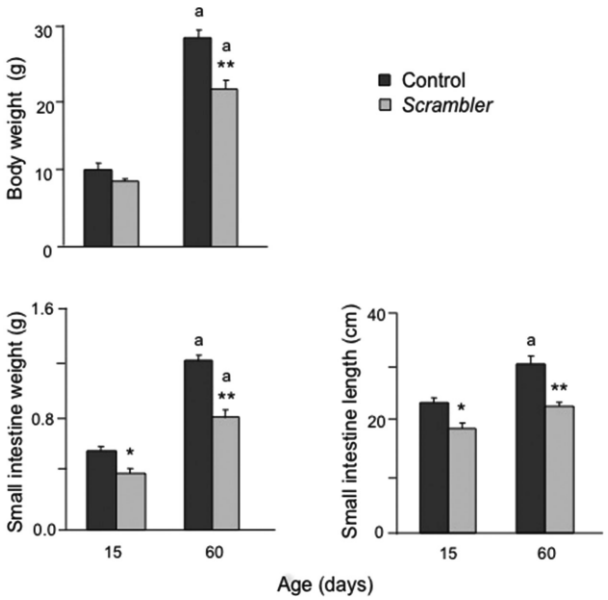

Figure 1 Body weight and small intestinal weight and length of control and *scrambler* mice

Data are presented as the means ± SEM of five different animals per age. One-way ANOVA showed an effect of age and mutation on body and small intestine weights ($P < 0.001$). Newman–Keuls' test $^{**}P < 0.001$ and $^{*}P < 0.05$ *scrambler versus* control mice, $^{a}P < 0.01$ *versus* 15 day-old mice.

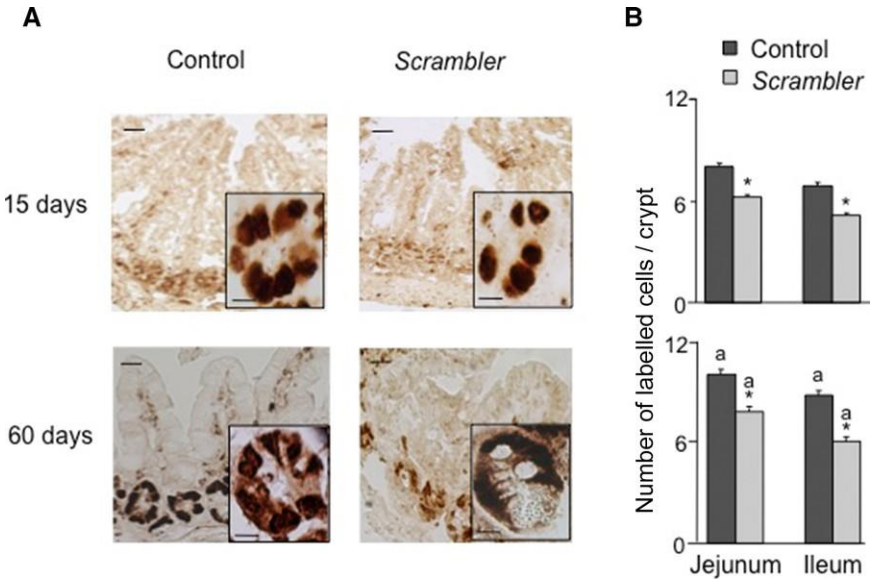

Figure 2 Cell proliferation rate in the intestinal epithelium of control and *scrambler* mice

The number of BrdU-labelled cells was determined with a monoclonal anti-BrdU antibody (1:300 dilution) in 30 well-oriented longitudinally crypts per mouse by light microscopy. Ten micrometre cryosections were used. (**A**) Representative sections of intestinal crypts. Scale bar = 25 and 10 μm in the inset. (**B**) Means ± SEM of the number of BrdU-labelled cells per crypt. The number of animals used per age was three *scrambler* and three control mice. One-way ANOVA showed an effect of mutation and age on cell proliferation ($P < 0.001$). Newman–Keuls' test: *$P < 0.001$ *scrambler versus* control mice, $^{a}P < 0.001$ *versus* 15day-old mice.

Table 1 | Morphometric parameters of small intestinal mucosa of *scrambler* and control mice

	Villi				Crypts			
	Height		Width		Depth		Diameter	
Mice	Jejunum	Ileum	Jejunum	Ileum	Jejunum	Ileum	Jejunum	Ileum
Age 15 days								
Control:	396 ± 9	199 ± 4	70 ± 1	58 ± 1	64 ± 2	54 ± 2	40 ± 1	36 ± 1
Scrambler:	323* ± 11	162* ± 6	72 ± 2	57 ± 1	60 ± 2	52 ± 2	39 ± 1	33 ± 1
Age 60 days								
Control:	483[a] ± 12	210[a] ± 3	80[a] ± 2	69[a] ± 3	77[a] ± 2	72[a] ± 1	46[a] ± 1	43[a] ± 1
Scrambler:	442*[a] ± 9	198*[a] ± 4	73* ± 2	57* ± 2	72[a] ± 2	70[a] ± 2	43[b] ± 1	43[a] ± 1

Means ± SEM of intestinal mucosa measurements (in μm). Five *scrambler* and five control mice per age were used. One-way ANOVA showed an effect of the age and of the mutation on intestinal morphology ($P < 0.001$). Newman-Keuls' test: *$P < 0.05$ *scrambler versus* control mice, [a]$P < 0.001$ and [b]$P < 0.05$ *versus* 15 day-old mice.

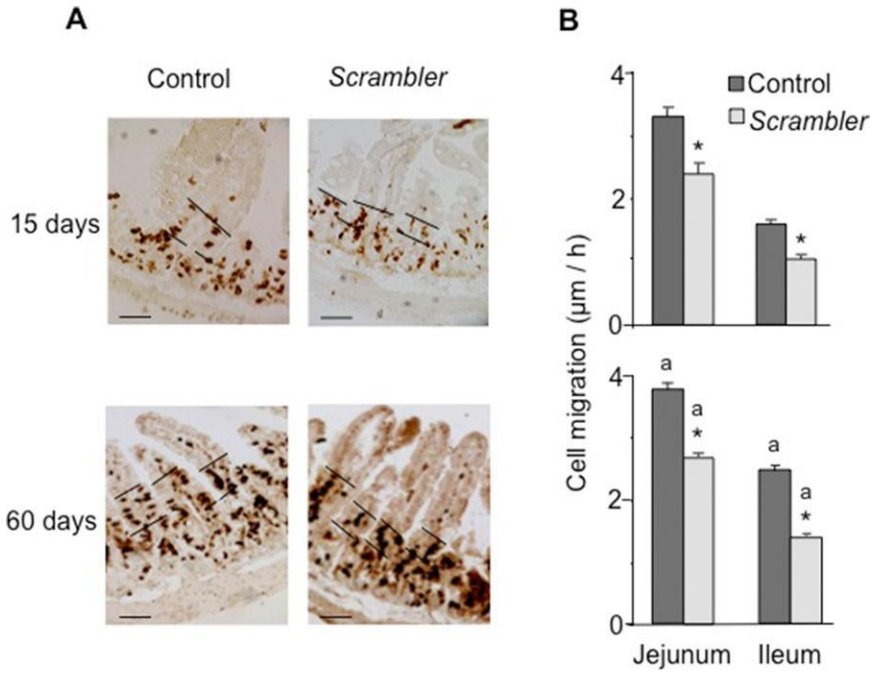

Figure 3 Cell migration rate in the intestinal epithelium of control and *scrambler* mice

The distance between the foremost BrdU-labelled cells and the base of the villi was measured and used to determine the cell migration rate. Ten micrometre cryosections were used. (**A**) Representative sections of mice intestine. Lines indicate the starting and the front point of labelled cells used to evaluate the enterocyte migration rate. Scale bar = 50 µm. (**B**) Means ± SEM of the distance (in µm) migrated per hour. The number of animals used per age was three *scrambler* and three control mice. One-way ANOVA showed an effect of both, mutation and age on cell migration rate ($P < 0.001$). Newman–Keuls' test: *$P < 0.001$ *scrambler versus* control mice, $^{a}P < 0.001$ *versus* 15 day-old mice.

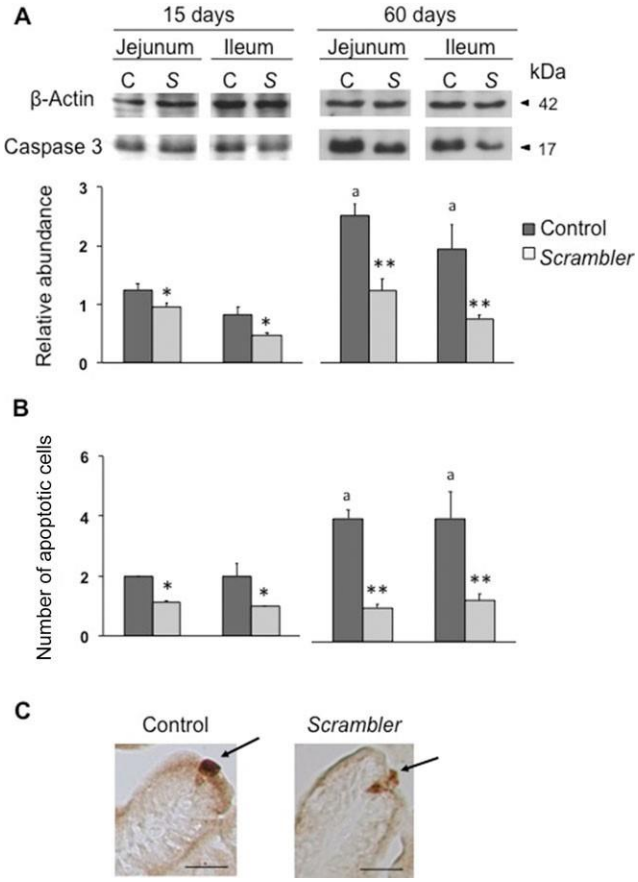

Figure 4 Cell apoptosis in the jejunum and ileum of control and *scrambler* mice

(A) Western blot analysis of intestinal cleaved Caspase-3 in control (C) and *scrambler* (S) mice. Fifty micrograms of protein were loaded to each lane. The dilution of the polyclonal anti-cleaved Caspase-3 antibody was 1:1000. Anti-*β*-actin antibody (1:3000 dilution) was used to normalise the bands. Histograms represent the means ± SEM of the relative abundance of the 17-kDa band.

(B) Ten micrometre cryosections of jejunum and ileum were incubated with anti-cleaved Caspase-3 antibody, 1:200 dilution, as described in the Materials and Methods section. 200 villi well oriented longitudinally per mouse were examined. Histograms represent the means ± SEM of the number of apoptotic cells per 40 villi. (**C**) Examples of apoptotic cells, indicated by the arrows, in the small intestine of control and *scrambler* mice. Scale bar = 25 μm. The number of animals used per age was three *scrambler* and three control mice. One-way ANOVA showed an effect of mutation and age on cell apoptosis ($P < 0.001$). Newman–Keuls' test: $^{**}P < 0.001$ and $^{*}P < 0.05$ *scrambler versus* control mice, $^{a}P < 0.001$ *versus* 15 day-old mice.

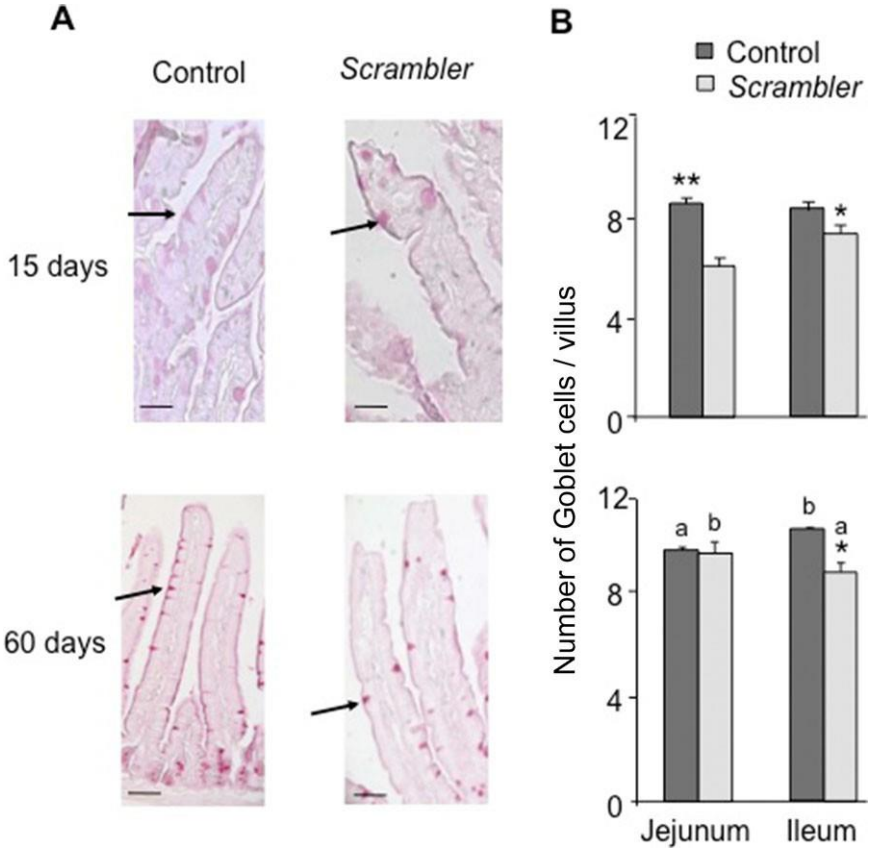

Figure 5 Number of Goblet cells in the intestinal epithelium of control and *scrambler* mice

Ten micrometre cryosections were stained with the PAS staining system. (**A**) Sections of the small intestine. Arrows indicate Goblet cells. Scale bar = 25 μm. (**B**) Means ± SEM of the number of Goblet cells per villus. The measurements were carried out in 30 villi well oriented longitudinally per mouse. The number of animals used per age was three *scrambler* and three control mice. One-way ANOVA showed an effect of mutation and maturation on the number of Goblet cells ($P < 0.001$). Newman-Keul's test: $^{**}P < 0.001$ and $^{*}P < 0.05$ *scrambler versus* control mice, $^{a}P < 0.001$ and $^{b}P < 0.05$ *versus* 15 day-old mice.

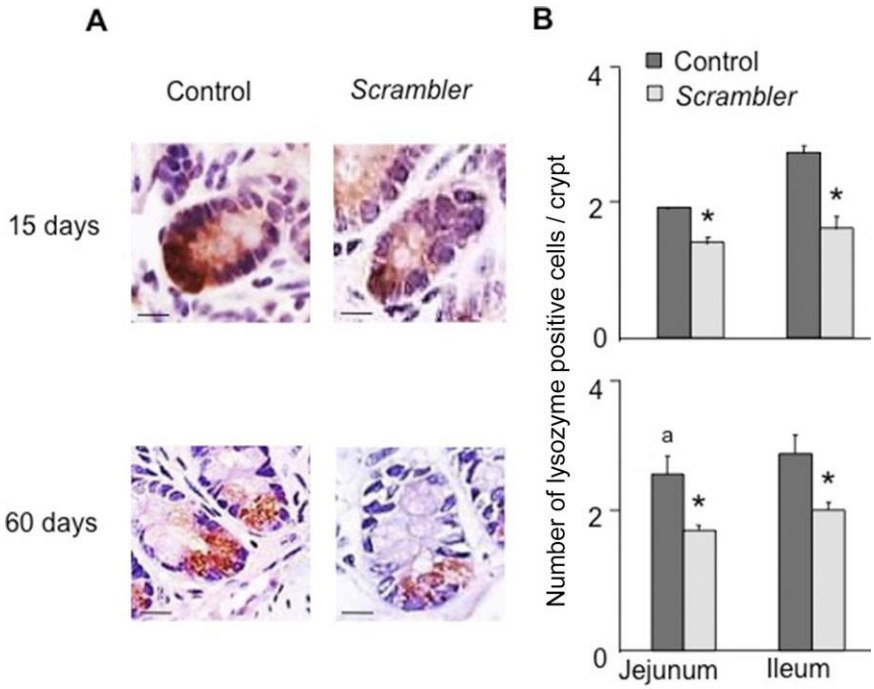

Figure 6 Number of Paneth cells in the epithelium of the small intestine of control and *scrambler* mice

The number of positive lysozyme cells was determined by immunohistochemistry as described in the Materials and Methods section. (**A**) Five micrometre paraffin sections of the small intestine. Sections were counterstained with hematoxylin. Scale bar = 10 μm. (**B**) Means ± SEM of the number of Paneth cells per crypt. The measurements were carried out in 30 crypts well oriented longitudinally per mouse. The number of animals used per age was three *scrambler* and three control mice. One- way ANOVA showed an effect of mutation and maturation on the number of Paneth cells ($P < 0.001$). Newman–Keuls' test:

*$P < 0.001$ *scrambler versus* control mice, $^{a}P < 0.001$ *versus* 15 day-old mice.

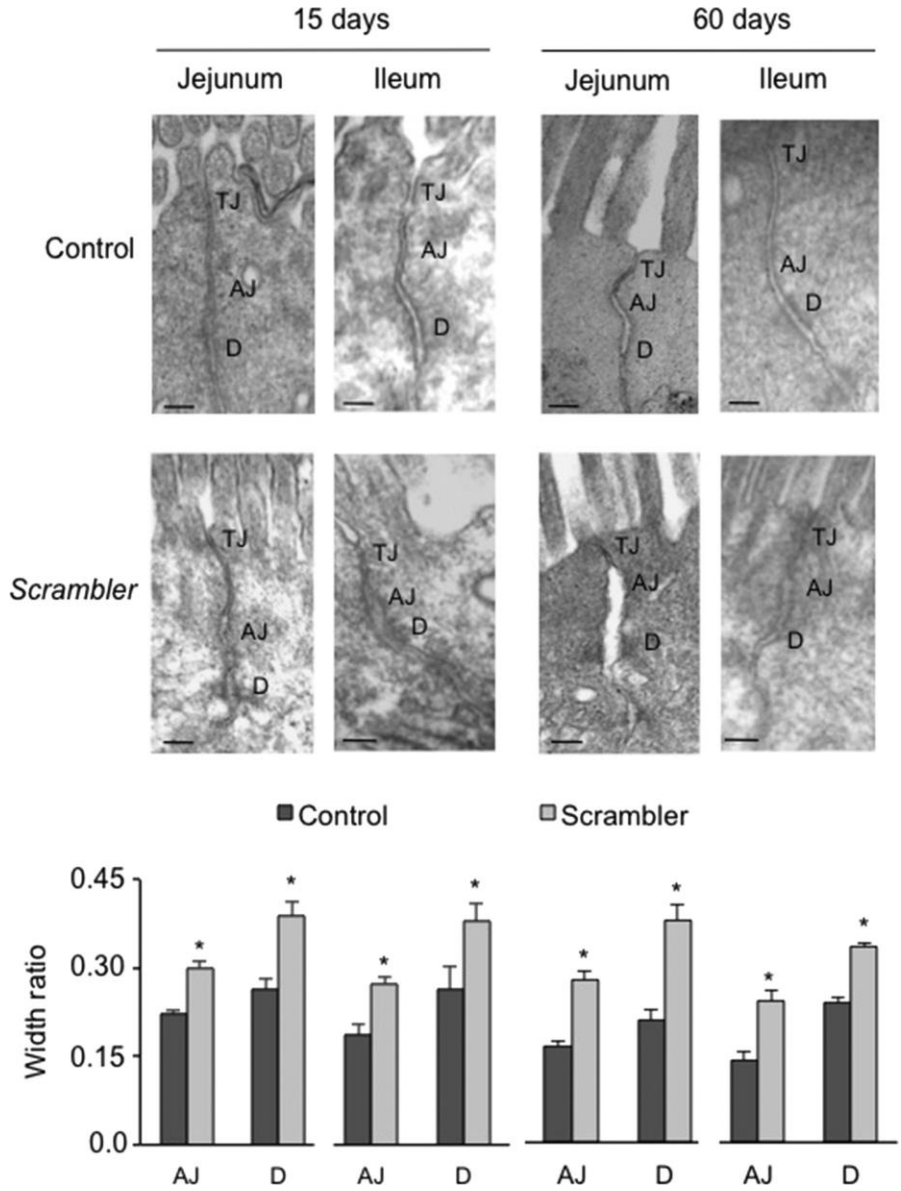

Figure 7 Electron microscopic images of intestinal apical membrane domain of control and *scrambler* mice

Apical cell-to-cell junctions of 15 and 60 day-old control and *scrambler* mice are shown. TJ, tight junction; AJ, adherens junction; D, desmosome. The histogram represents the average of junctions width/microvilli width ratio. Six to eight junctions were examined per type of mouse. The microphotographs are representative of three different assays performed on three *scrambler* and three control mice. Scale bar = 100 nm. Student's *t* test: **P* < 0.001 *scrambler versus* control mice.

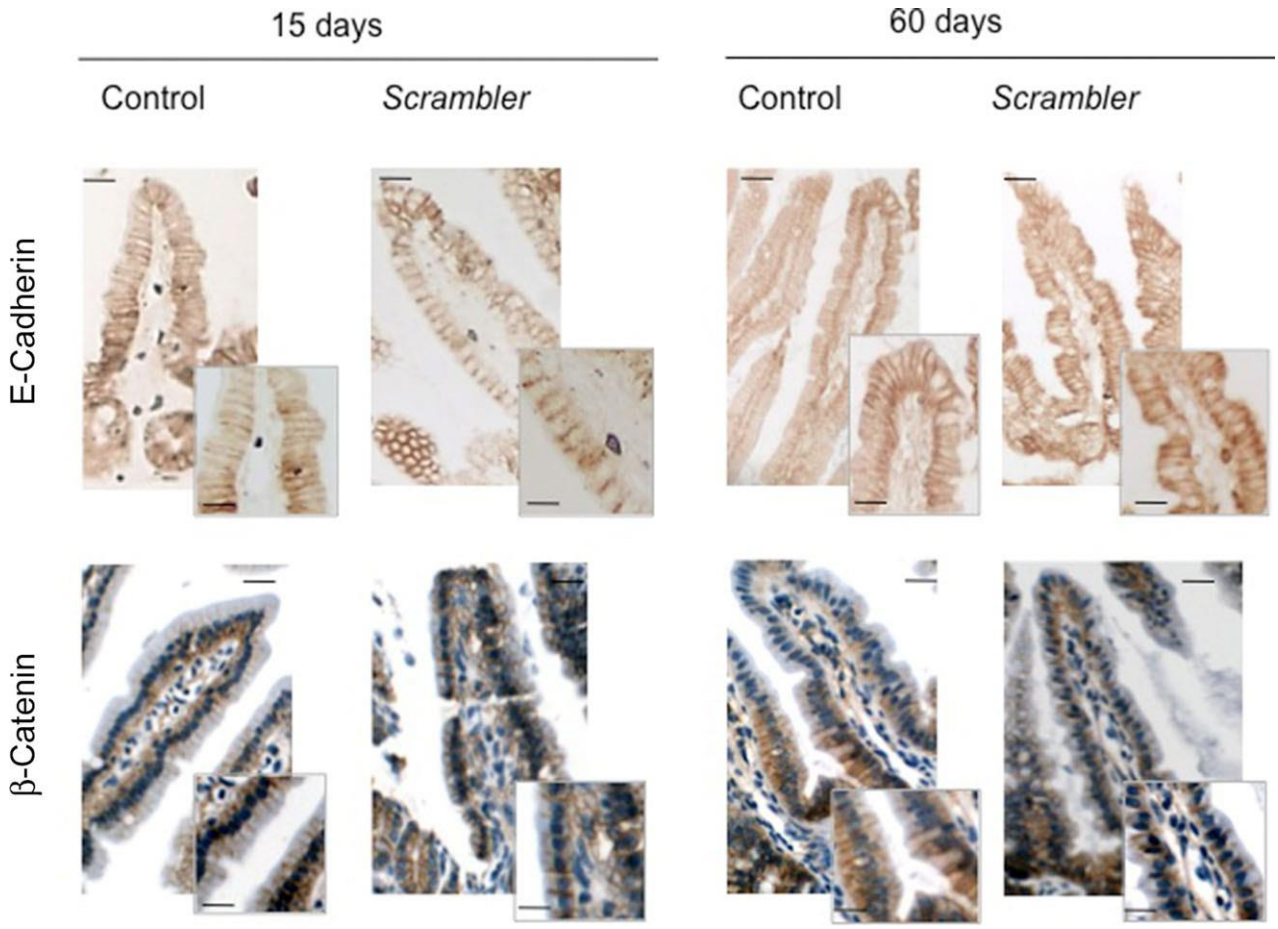

Figure 8 Immunolocalisation of E-cadherin and *β*-catenin in the intestinal epithelium of control and *scrambler* mice

Five micrometre paraffin sections of jejunum and ileum obtained from 15 and 60 day-old mice were incubated with either anti- E-cadherin (1:500 dilution) or anti-*β*-catenin (1:100 dilution) antibodies. Sections showing *β*-catenin were counterstained with hematoxylin. Scale bar = 20 and 50 μm in the insets. The photographs are representative of three different assays performed on three *scrambler* and three control mice.

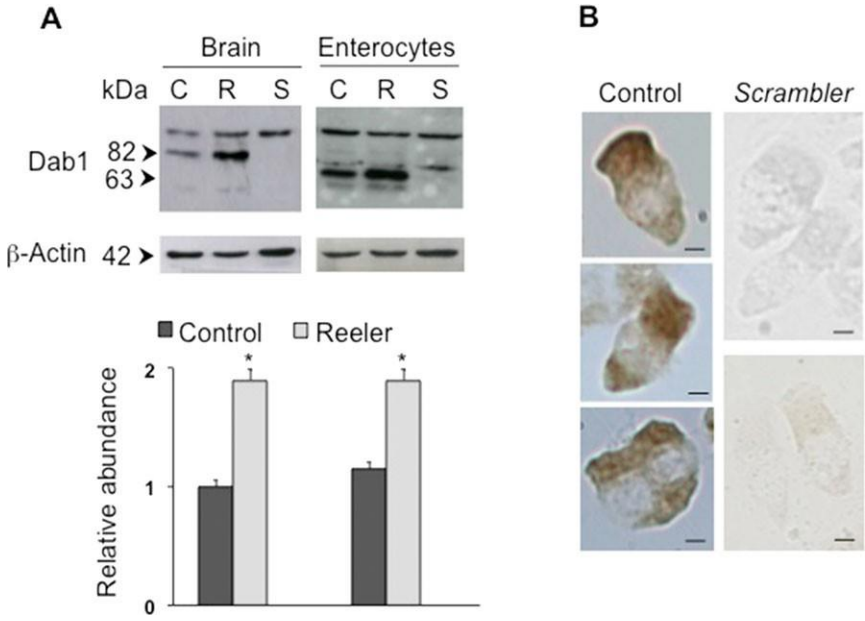

Figure 9 Immunological assays of Dab1 in enterocytes of control, *reeler* and *scrambler* mice

Sixty day-old control, *reeler* and *scrambler* mice were used. (**A**) Western blot analysis of Dab1. Fifty micrograms of protein extracted from either enterocytes or brain of control (C), reeler (R) and *scrambler* (S) mice were loaded to each lane. The blots were probed with anti-Dab1 antibody (ABR, 1:3000 dilution) as described in the Materials and Methods section. Anti-*β*-actin antibody (1:3000 dilution) was used as a control of protein loading. Histograms represent the means ± SEM of the relative abundance of the 82 and 63 kDa bands. The blot is representative of three different assays performed on three *reeler*, three

scrambler and three control mice. (**B**) Enterocytes of control and *scrambler* mice were incubated with anti-Dab1 antibody (AbCam, 1:100 dilution) as described in the Materials and Methods section. Scale bars = 2 μm. The photographs are representative of three different assays performed on three *scrambler* and three control mice.